Charge/mass yields in the fission of highly excited heavy actinides

*H.*Pașca[1,2,*], *A. V.* Andreev[1], *G. G.* Adamian[1], and *N. V.* Antonenko[1]

[1]Joint Institute for Nuclear Research, 141980 Dubna, Russian Federation
[2]"Babeş-Bolyai" University, Faculty of Physics, 400084 Cluj-Napoca, Romania

Abstract. The charge (mass) distributions of fission fragments resulting from low- and high-energy fission of the isotopes of Fm and No are studied with the statistical scission-point fission model. The calculated results are compared with the available experimental data. The transformation of the shape of the charge distribution with increasing isospin and excitation energy occurs gradually. At some critical excitation energy the the saturation of the symmetric component of the charge (mass) yield is demonstrated.

1 Introduction

The mass distributions in low-energy fission of nuclei U–Cf are known to be mostly asymmetric [1]. The first observation of the onset of symmetric distribution was made in the spontaneous fission of ^{257}Fm [1, 2]. For ^{258}Fm, the spontaneous fission results in the unexpected narrow symmetric mass distribution [3]. The symmetric distributions have been also observed in the spontaneous fission of ^{259}Fm, ^{259,260}Md, ^{258,262}No, and ^{259}Lr [1]. The thermal-neutron-induced fission of ^{256,257}Fm [1] leads to the symmetric mass distribution, but with larger width than that in spontaneous fission of ^{258}Fm. For spontaneous fissioning Fm isotopes, an evolution of mass-yield shape with increasing isospin occurs suddenly as demonstrated in Ref. [3]. However, a survey of literature reveals a lack of data on the charge distributions of fission products in the spontaneous and induced fission of Fm and No particularly as a function of isospin and excitation energy.

In this short work, we employ the improved version of the statistical scission-point model [4], to study the evolution of the charge (mass) distribution of fission fragments with increasing mass number and excitation energy of even-even isotopes of $^{254-260,264}$Fm and $^{258-264}$No. Our aim is to predict the transformation of the shape of charge distribution with increasing neutron number and excitation energy.

2 Model

The statistical scission-point model [4] relies on the assumption that the statistical equilibrium is established at scission of fissioning nucleus where the observable characteristics of fission are formed. The model [5] is shown to be well suited for describing the scission configuration. Thus, the fissioning nucleus at scission-point is modeled by two nearly touching coaxial ellipsoids - fragments of the DNS with mass (charge) numbers A_L (Z_L) and A_H (Z_H) for the light (L) and heavy (H) fragments, respectively. Here, $A = A_L + A_H$ ($Z = Z_L + Z_H$) is the mass (charge) number of fissioning nucleus. By taking into consideration the volume conservation, the shape of the system is defined by the mass and charge numbers of the fragments, the deformation parameters β_i ($i = L, H$), and interfragment distance R. The potential energy [4] of the DNS consists of the energies of the fragments (the liquid-drop energy U_i^{LD} plus deformation dependent shell-correction term δU_i^{shell}) and energy $V = V^C + V^N$ of the fragment-fragment interaction. The interaction potential consists of the Coulomb interaction potential V^C of two uniformly charged ellipsoids and nuclear interaction potential in the double-folding form.

$$\begin{aligned} U(A_i, Z_i, \beta_i, R) &= U_L^{LD}(A_L, Z_L, \beta_L) \\ &+ \delta U_L^{shell}(A_L, Z_L, \beta_L, E_H^*) + U_H^{LD}(A_H, Z_H, \beta_H) \\ &+ \delta U_H^{shell}(A_H, Z_H, \beta_H, E_H^*) + V^C(A_i, Z_i, \beta_i, R) \\ &+ V^N(A_i, Z_i, \beta_i, R). \end{aligned} \quad (1)$$

In the region of fission fragments considered, the interaction potential has a potential pocket and external barrier located at the distances of about (0.7–1.1) fm and (1.5–2) fm, respectively, between the tips of the fragments depending on deformations of the fragments. The internuclear distance R in Eq. (1) corresponds to the position $R = R_m(A_i, Z_i, \beta_i)$ of the minimum of this pocket. The decay barrier, $B_{qf}(A_i, Z_i, \beta_i)$, calculated as the difference of the potential energies at the bottom of the potential pocket [$R = R_m(A_i, Z_i, \beta_i)$] and the top of the external barrier [$R = R_b(A_i, Z_i, \beta_i)$], prevents the decay of the DNS in R.

Because the thermal equilibrium is assumed at scission point, the excitation energy $E^*(A_i, Z_i, \beta_i, R_m) = E^*(A_i, Z_i, \beta_i, R_m) = E^*_{CN} + [U_{CN}(A, Z, \beta) - U(A_i, Z_i, \beta_i, R_m)]$ at scission is calculated as the initial excitation energy of the fissioning nucleus E^*_{CN} plus the difference between the potential energy $U_{CN}(A, Z, \beta)$ of the fissioning nucleus and

*e-mail: pasca@theor.jinr.ru

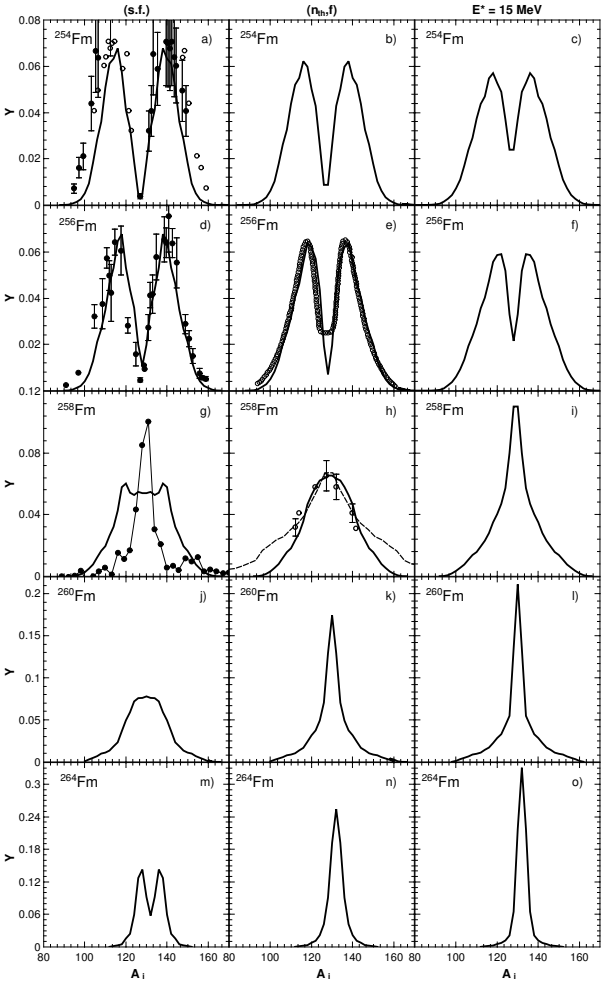

Figure 1. The calculated mass distributions (solid lines) resulting from the spontaneous (E^* = 0 MeV, the first column) and induced (E^* = 15 MeV, the third column) fission of the indicated nuclei ^{254,256,258,260,264}Fm, and thermal-neutron-induced ($E^* \sim 6.3$ MeV, the second column) fission of nuclei ^{253,255,257,259,263}Fm. The open symbols represent experimental data of Refs. [3, 6–9]. The spontaneous fission data for the ^{258}Fm were multiplied by the factor 0.8. In panel h), the dashed line represents the provisional mass deduced in Ref. [9], and the open square represent radiochemically deduced secondary yield, while the open circles are the derived primary distributions [7].

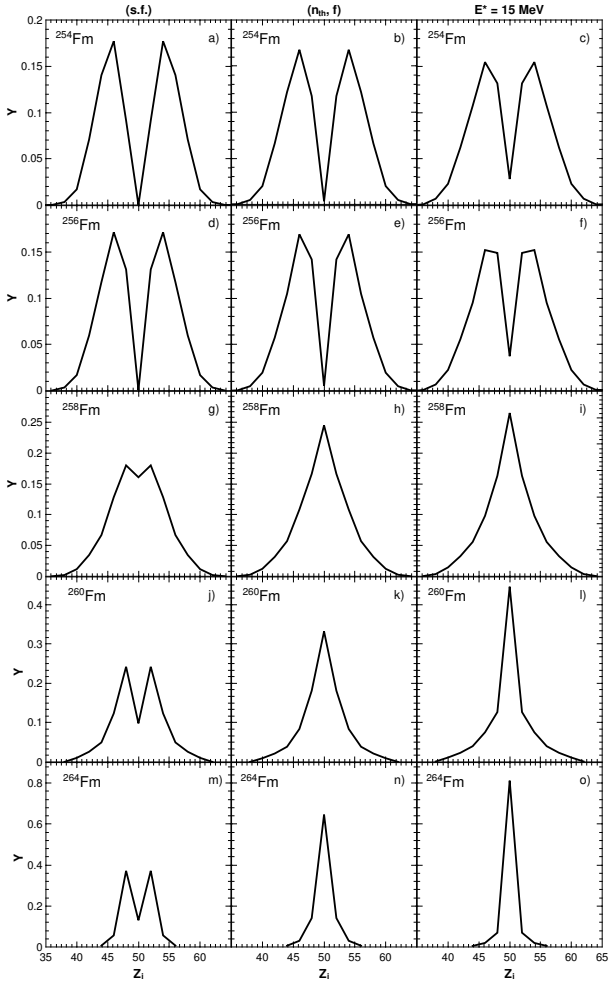

Figure 2. The calculated charge distributions (solid lines) resulting from the spontaneous (E^* = 0 MeV, the first column) and induced (E^* = 15 MeV, the third column) fission of the indicated nuclei ^{254,256,258,260,264}Fm, and thermal-neutron-induced ($E^* \sim 6.3$ MeV, the second column) fission of nuclei ^{253,255,257,259,263}Fm.

one $U(A_i, Z_i, \beta_i, R_m)$ of the system at the scission point [4]. The excitation energies E_i^* in the DNS nuclei are assumed to be shared between the fragments proportionally to their masses.

The shell correction terms are calculated with the Strutinsky method and the two-center shell model [4]. The damping of these terms with excitation energy E_i^* is introduced as: $\delta U_i^{shell}(A_i, Z_i, \beta_i, E_i^*) = \delta U_i^{shell}(A_i, Z_i, \beta_i, E_i^* = 0) \exp[-E_i^*/E_D]$. The relative formation-decay probability of the DNS with particular masses, charges and deformations of the fragments is statistically calculated as follows [4]:

$$w(A_i, Z_i, \beta_i, E^*) = N_0 \exp\left[-\frac{U(A_i, Z_i, \beta_i, R_m) + B_{qf}(A_i, Z_i, \beta_i)}{T}\right], \quad (2)$$

where N_0 is the normalization factor, t is the temperature calculated as $T = \sqrt{E^*/a}$, and $a = A/12$ MeV^{-1} is the level density parameter in the Fermi-gas model. The term $\exp\left[-B_{qf}(A_i, Z_i, \beta_i)/T\right]$ describes the decay probability of the system.

The mass-charge distribution of fission fragments are obtained by integrating Eq. (2) over β_L and β_H

$$Y(A_i, Z_i, E^*) = N_0 \int d\beta_L d\beta_H w(A_i, Z_i, \beta_i, E^*). \quad (3)$$

For the calculations of mass and charge distributions, one should sum $Y(A_i, Z_i, E^*)$ over Z_i and A_i, respectively. As follows, the yield with mass A_L (charge Z_L) depends on the number of fragmentations with the same A_L (Z_L) but different Z_L (A_L).

The calculations were restricted only to even-even fission fragments which mainly define the shapes of the charge and mass distributions. The even-odd effects would add some oscillations to this smooth part. The details of the calculations are prezented in full in [4]. At energies considered, we assume that the neutron emission prior to fission will not cause major change in the fission yield of isotopes of Fm and No.

The explanation of the asymmetric fission mode at high excitations by the multi-chance fission or fission after

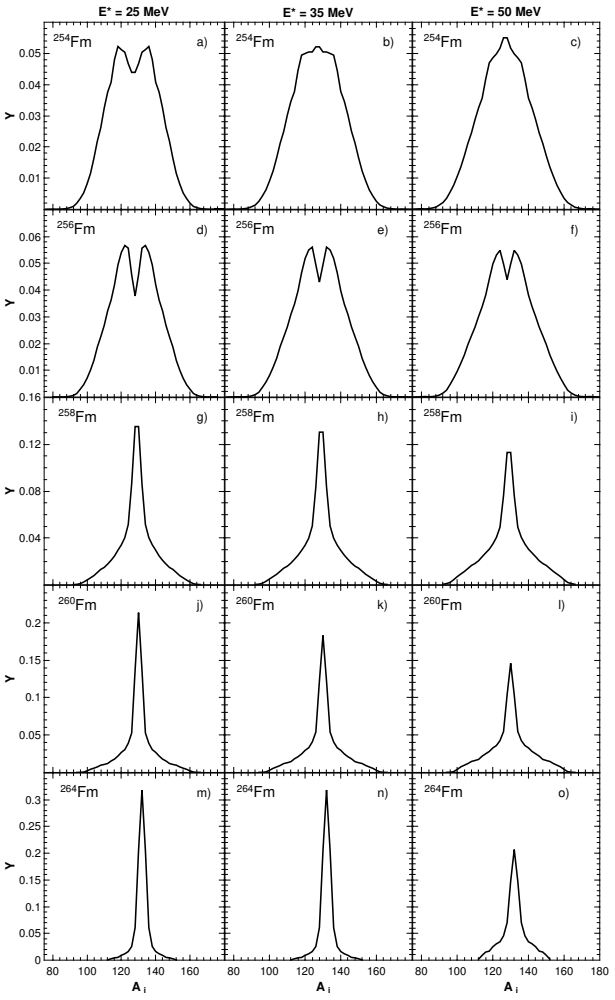

Figure 3. The same as in Fig. 1, but for E^* = 25 MeV [the first column], E^* = 35 MeV [the second column], and E^* = 50 MeV [the third column] excitation energies.

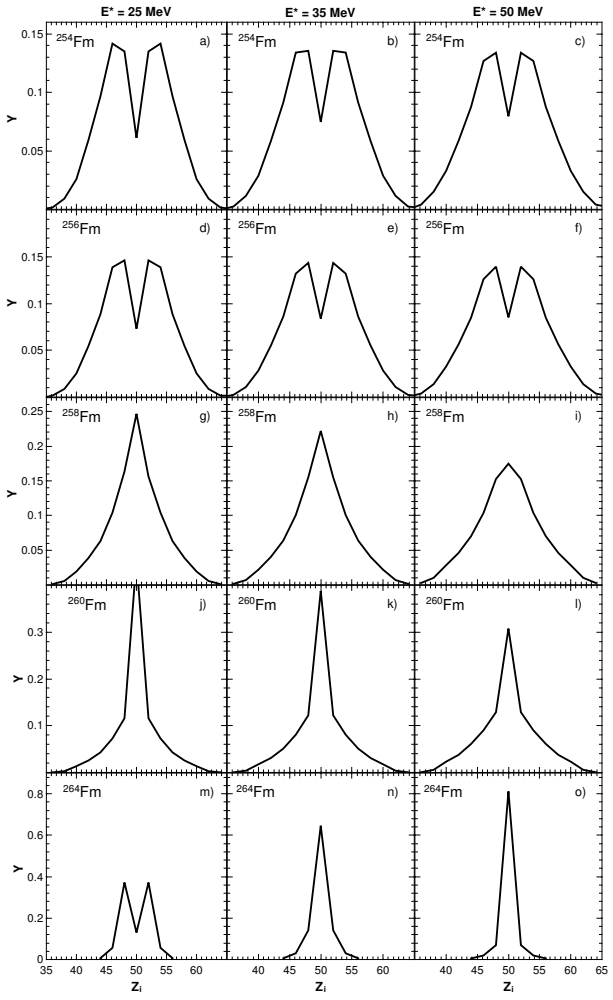

Figure 4. The same as in Fig. 2, but for E^* = 25 MeV [the first column], E^* = 35 MeV [the second column], and E^* = 50 MeV [the third column] excitation energies.

consecutive neutron evaporations is strongly model dependent and under discussion. As known from the experimental data [10], the number of pre-scission neutrons does not exceed 1–2 at excitation energies 50–60 MeV of heavy actinides. In nuclei considered the estimated fission barrier is smaller than neutron separation energy. Thus, the role of multi-chance fission is expected to be suppressed in these nuclei.

3 Results and discussions

In Figs. 1-6, the calculated mass and charge distributions resulting from the spontaneous and induced fission of ^{254,256,258,260,264}Fm and ^{258,260,262,264}No isotopes are presented. The measured mass distributions [6–9] are well reproduced for the spontaneous fission of ^{254,256}Fm and ^{262}No and for the thermal-neutron-induced fission of ^{255,257}Fm. In the cases of fission of ^{254,256}Fm, the measured mass distributions present two asymmetric peaks as in our theoretical results. In contrast to the experimental data [3], the calculated mass distribution for ^{258}Fm is rather wide and has asymmetric bumps, even though the symmetric yields are extremely enhanced, and is strikingly similar to the experimental one for ^{257}Fm (Fig. 1) [2]. For ^{258}No (Figs. 3-4), the symmetric mass-yields are larger than the asymmetric mass-yields that is in a good agreement with the experimental data [3].

The calculated charge distributions of spontaneous fission of ^{254,256,258,260,264}Fm have the asymmetric shape (Figs. 1-2). The tendency to a more symmetric charge splitting of fermium isotopes with increasing neutron number is clearly seen. In the case of the spontaneous fission of ^{258}Fm (Figs. 1-2), the charge distribution presents two peaks, with a small minimum for the symmetric Sn + Sn charge split. This is explained by the fact that the high yield of Cd (Z_L=48) or Te (Z_H=52) mainly originates from three mass fragmentations ^{122}Cd + ^{136}Te, ^{124}Cd + ^{134}Te, and ^{126}Cd + ^{132}Te which have almost the same potential energies U.

In the case of spontaneous fission of ^{260}Fm with the symmetric mass distribution, the charge distribution is asymmetric one with charge split Cd + Te. With increasing excitation energy the charge distribution becomes symmetric one (Figs. 1-2 and 3-4). For the thermal-neutron-induced fission of ^{257}Fm , the experimental and calculated mass distributions are symmetric ones whereas the predicted charge distribution is asymmetric. However, at $E^* \geq 15$ MeV the difference between these distributions

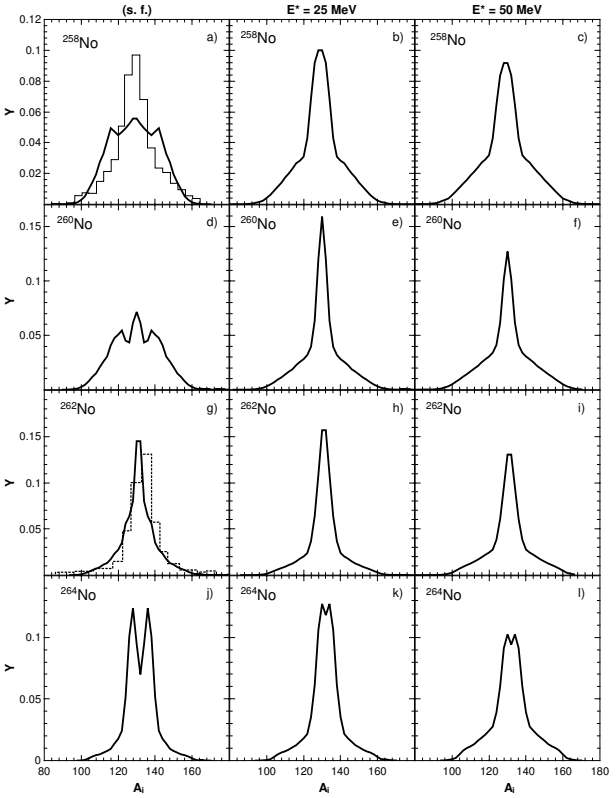

Figure 5. The calculated mass distributions (solid lines) resulting from the fission of the indicated nuclei ^{260,262,264}No at excitation energies E^* = 0 MeV [the first column], E^* = 25 MeV [the second column], and E^* = 50 MeV [the second column]. In panels a) and g), the histograms represent experimental data of Refs. [3] and [11], respectively.

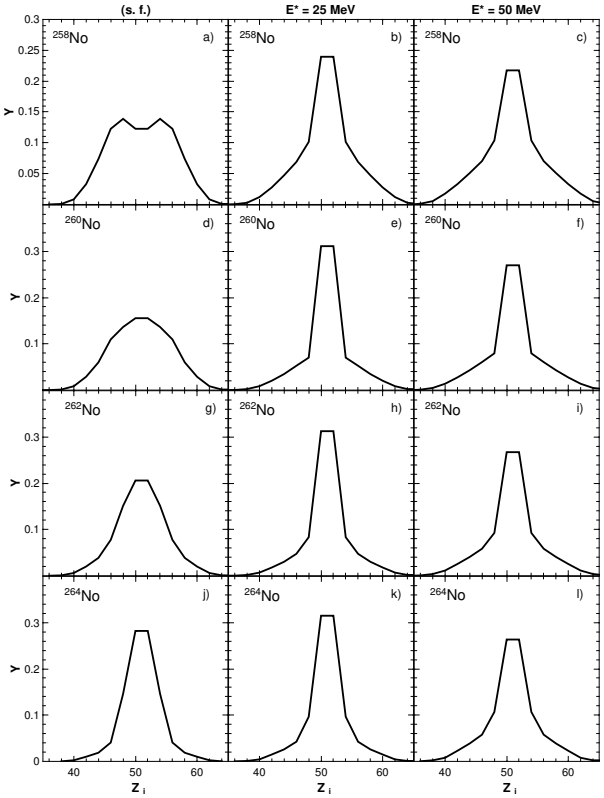

Figure 6. The calculated charge distributions (solid lines) resulting from the fission of the indicated nuclei ^{260,262,264}No at excitation energies E^* = 0 MeV [the first column], E^* = 25 MeV [the second column], and E^* = 50 MeV [the third column].

vanish. For the induced fission of ^{254}Fm at E^* =35 and 50 MeV , the shape of mass yields becomes symmetric in contrast to one of the charge distribution. This unexpected difference between the shapes of mass and charge yields is worth to be studied experimentally.

In the case of spontaneous fission of ^{260}No (Figs. 5-6), the mass distribution displays symmetric ($A_L = A_H = 130$) and asymmetric ($A_L = 122$, $A_H = 138$) peaks. For ^{260}No, the peaks of the charge distribution are at $Z_L = 50$ and $Z_H = 52$. The spontaneous fission of ^{264}No has the slightly asymmetric mass distribution with peaks at $A_L = 128$ and $A_H = 136$ and charge distribution with peaks at $Z_L = 50$ and $Z_H = 52$. Note, that in the case of spontaneous fission of ^{264}Fm, the peaks of charge and mass distributions are at $Z_L = 48$, $Z_H = 52$ and $A_L = 128$, $A_H = 136$, respectively.

The interplay between the liquid-drop surface energy and the nucleus-nucleus interaction potential at scission is the main reason of the appearance or disappearance of the asymmetric fission mode. This interplay depends on the shell effects, excitation energy, and isospin of the fissioning nucleus. The shell effects affect directly and indirectly (through the deformations of nuclei) the appearance of the asymmetric minimum.

As a global trend for the isotopes of Fm and No, the symmetric components of the mass- and charge-yields are enhanced with increasing excitation energy (Figs. 1-6). The saturation of the symmetric components is reached at around 15–30 MeV. At larger E^* the distributions only become wider. The fission of ^{260}No is a good example of that. The shift to more symmetric mass and charge distributions and the saturation of the symmetric components with increasing excitation energy can be understood in the following way: for each mass and charge fragmentation the configurations with the highest yields correspond to local minima on the potential energy surfaces (β_L, β_H). These minima of the potential energy surface (PES) result from the subtle competition between the macroscopic interaction and liquid-drop (surface) energies, and the microscopic shell corrections at scission. The strong shells also affect the macroscopic parts of the potential energy by fixing the minimum energy at small deformations (β_L, β_H). With increasing excitation energy, the shell effects are washed out, and the stiffness of the nuclear surface decreases. The combined effect is the enlargement of the minima on the PES and their shift towards much larger deformations. At large E^* the shell effects are completely damped, the surface stiffness becomes minimal, and the minima on the PES reach their maximum widths and final position. At this point the yields reach the maximal values, and further increase of excitation energy leads only to the population of more asymmetric accessible configurations.

4 Conclusions

The mass and charge distributions resulting from the spontaneous and induced fission of even-even nuclei ^{254,256,258,260,264}Fm and ^{258,260,262,264}No were calculated within the statistical scission-point fission model. For

these fissioning nuclei, the available experimental mass distributions in the spontaneous and thermal-neutron-induced fission were well described excepting ^{258}Fm(s.f.). In contrast to the experimental data, the calculated mass distribution for the spontaneous fission of ^{258}Fm is rather wide and has asymmetric bumps, even though the symmetric yields are extremely enhanced. However, the calculated spontaneous fission of ^{258}Fm shows slightly asymmetric charge distribution. In the case of spontaneous fission of ^{260}Fm, we found that the mass distribution is symmetric but the charge distribution are asymmetric (Z_L = 48, Z_H = 52). For ^{260}No(s.f.), the mass distribution has asymmetric and symmetric peaks and the charge distribution has peaks at Z_L = 50 and Z_H = 52.

For the thermal-neutron-induced fission of ^{257}Fm, the asymmetric charge distribution (Z_L=48, Z_H=52) was predicted. As well-known, the reaction ^{257}Fm(n_{th},f) has the symmetric mass-yield. For the fission of ^{254}Fm at E^* =35 and 50 MeV, the symmetric shape of mass-yields and the asymmetric shape of charge-yields were obtained. For ^{260,262,264}No the asymmetric peaks at Z_L=50 and Z_H=52 (Z_L=50 and Z_H=54) is conserved with increasing E^*. The experimental verifications of these theoretical predictions are desirable.

Our calculations for spontaneously fissioning nuclei Fm and No suggest that an evolution of charge-yield shape occurs gradually with increasing isospin and excitation energy. For the isotopes of Fm and No, the symmetric components of mass and charge distributions are enhanced with increasing E^*. For the first time, we demonstrated that at some critical E^* the saturation of the symmetric yields occurs. For ^{254,256}Fm, the shape of charge-yields evolves slower with increasing E^* than the shape of the mass-yields and remains asymmetric even at high excitation energy (E^* = 50 MeV). In the fission of ^{258}Fm and ^{260}Fm, the symmetric component of the charge (mass) distribution is enhanced much faster with excitation energy due to the rapid transition from the strong shell-effect-governed to the macroscopic-governed symmetric fission behavior. Once the shell effects are damped at high excitation energy, the fission is strictly driven by the competition between the liquid-drop binding energy and the interaction energy of the two fragments. Any increase of excitation energy leads to the access of previously inaccessible asymmetric configurations. This, together with the smooth character of macroscopic energies, mainly leads to a saturation of the symmetric yields with increasing excitation energy and broadening of the mass and change distributions. Thus, the evolution of charge and mass distributions with the variation of excitation energy and isospin is related to the change of the PES at scission. The saturation effect is worth to be studied experimentally.

References

[1] D.C. Hoffman *et al.*, Phys. Rev. C **41**, 631 (1990); D.C. Hoffman, J. of Alloys and Compounds **213/214**, 67 (1994); S. Hofmann and G. Münzenberg, Rev. Mod. Phys. **72**, 733 (2000); A.N. Andreyev, M. Huyse, and P. Van Duppen, Rev. Mod. Phys. **85**, 1541 (2013)

[2] E.K. Hulet *et al.*, Phys. Rev. C **21**, 966 (1980)

[3] E.K. Hulet *et al.*, Phys. Rev. C **40**, 770 (1989)

[4] H. Paşca, A.V. Andreev, G.G. Adamian, N.V. Antonenko, Phys. Rev. C **94**, 064614 (2016); Phys. Lett. B **760**, 800 (2016); Nucl. Phys. **A969**, 226 (2018)

[5] G.G. Adamian, N.V. Antonenko, and W. Scheid, Lect. Notes Phys. **848**, *Clusters in Nuclei*, Vol. **2**, Ed. by Christian Beck (Springer-Verlag, Berlin, 2012) p. 165.

[6] K.F. Flynn *et al.*, Phys. Rev. C **5**, 1725 (1972)

[7] K.F. Flynn *et al.*, Phys. Rev. C **12**, 1478 (1975)

[8] R.M. Harbour *et al.*, Phys. Rev. C **8**, 1488 (1973)

[9] W. John *et al.*, Phys. Rev. Lett. **27**, 45 (1971); R.C. Ragaini *et al.*, Phys. Rev. C **9**, 399 (1974)

[10] D. Hilscher and H. Rossner, Ann. Phys. (France) **17**, 471 (1992)

[11] R.W. Lougheed *et al.*, *Proceeding of the 3rd Chemistry Congress of North America* (Toronto, Canada, 1988); *Nuclear Chemistry Division FY-1988 Annual Report* (Lawrence Livermore National Laboratory, UCAR-10062-88, 1988), p. 135